第2節 リポソームの固体微粒子との複合化とエレクトロ・パーミエーション

1. はじめに

リポソームは脂質二分子膜の微粒子であり，その内部の液相や膜内に種々の生体機能性分子を保持できるため薬物を配達するキャリアとして研究されている。このリポソームと他の微粒子を組み合わせることにより高機能を持つ複合微粒子の開発が可能である。例えば，任意の場所で任意の時間に薬物を放出・供給するツールの開発も可能であろう。

我々が病気になったとき，すなわち，組織細胞が正常でなくなったときにその回復のため薬をなんらかの手段で病細胞まで送る。通常行われる薬物輸送の方法にはいくつかある。一つは口から内服し消化器や粘膜から，あるいは静脈注射にて血管系に入れ毛細血管から組織細胞へ送る方法。一つは皮下注射や湿布により直に患部へ送る方法である。

先の一番目の方法で患部だけに集中的に薬物を投与することを目指すには，薬物を内包するカプセル(リポソームなど)の表面に患部細胞にだけ結合(認識)する分子を付けて利用することである。これはミサイル試薬とも呼ばれ研究展開されている。一方，リポソームを先の二番目の方法に利用することも可能であろう。疾患部の場所がはっきりしているときにはそこだけに薬を投与すれば十分であるし，余分な副作用も少なくなるはずである。例えば，リポソーム微粒子と磁性微粒子との複合体を用いれば，磁性針によりその存在場所のコントロールができ，針電極を用いて電場を印加することにより，リポソーム内部に保持していた薬物の局部放出を可能にするであろう。近年，X線CTやMRIなどの物理検査法により体内の病巣の場所がより詳細に分かるようになってきている。外科的手法と内科的手法のドッキングは有用な方法であると考えられる。これまでも，薬物療法において注射器を用いて薬物を直に患部へ投与することと物理的手法とを組み合わせたものが研究されてきた。その一つに，エレクトロ・ケモセラピーという方法がある。これはパルス電場のアシストで細胞膜を通して薬を細胞内へ輸送する方法である。とくに表層癌治療に有効で治癒率が90％以上を超える成果をあげているそうである。通常の有効濃度より低い濃度で効果が期待できるため副作用防止をも期待される。これにリポソーム系を利用することは十分可能であろう。

ここでは，上記の視点から，リポソームと固体微粒子からなる複合化微粒子の作製法とリポソーム膜の電場による物質透過能変化についての研究を紹介する。

2. リポソームと固体微粒子の複合微粒子

2.1 金平糖型複合粒子作製の指針

1個の固体微粒子を中心に，その周りにリポソーム粒子が複数個付着した金平糖型複合微粒子の作製について述べる。構造の基本となる中心固体微粒子は単一粒子として溶液中に安定分散している必要がある。これを実現するには粒子間に強い反発力が働いていなければならない。これには粒子表面の電気二重層間反発力や水和反発力が利用される。種々の粒子のなかでシリカ粒子は表面解離基-OHがあるため，この二つの特性を持ち非常によく水系に分散する粒子である。一方，周囲に付けるリポソーム粒子も単一粒子として分散していなければならない。種々の脂質から形成されるリポソームの多くは単一粒子として分散性のよいものである。親水基側に水

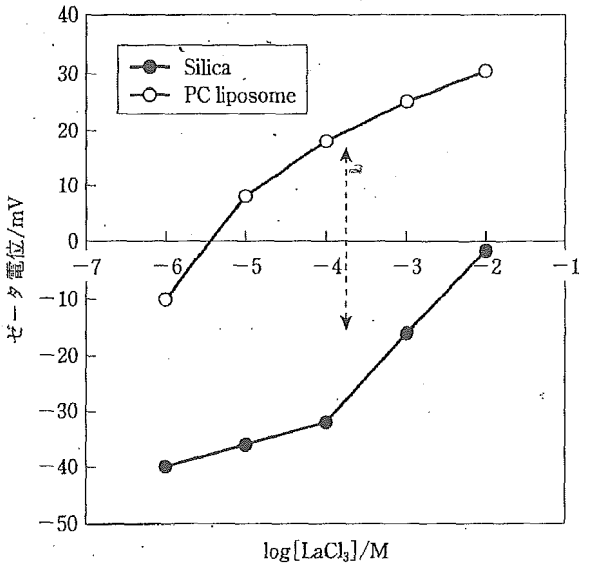

図1　シリカ粒子とPCリポソーム(負荷電の不純物を含む)のゼータ電位の塩化ランタン濃度依存性

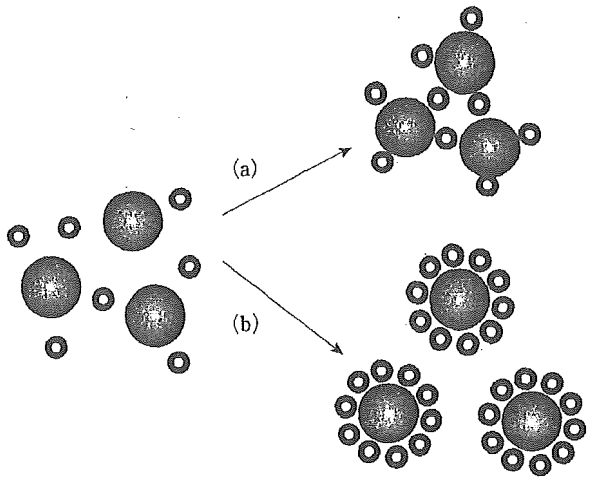

図2　大きな凝集体(フロック)の形成(a)と金平糖型複合粒子の形成(b)

和性のコリンを持つ脂質と電荷を持つ脂質の混合系は分散性の点からはとくに良い。これらの一次粒子からの複合微粒子の作製においては，中心微粒子と周辺微粒子との接合(会合)が必要であるが，その条件設定にはコロイド科学における異種粒子間の相互作用(ヘテロ凝集)の概念が利用できる。すなわち，2種類の微粒子が存在する系の溶液条件には同種粒子間には反発力が，異種粒子間には引力が生ずる条件を利用する。電気二重層間相互作用を利用するときは，単に異種粒子表面がそれぞれ反対符号に帯電しているだけでは不十分である。なぜならば，相互作用力が引力になるか反発力になるかは，両者の電気二重層が重なったときどのように電気二重層エネルギーが緩和されるかに依存するからである。簡便には両者の持つ表面電位(あるいはゼータ電位)がある程度大きくそれぞれ正負の電位を持ち，同程度の大きさである点を選ぶと良い。例えば，図1はシリカ微粒子とPCリポソーム(Sigma社のegg phosphatidylcholine，負荷電の不純物を含む)の場合に塩化ランタン水溶液での両粒子が持つゼータ電位であるが，塩化ランタン濃度10^{-4}M付近で両粒子は正と負で同程度の電位を示す。この条件で粒子間は引力になりヘテロ凝集は進行する。また，カチオン性脂質をリポソームに混入しヘテロ凝集の条件を実現することもできる。

きれいな金平糖型複合粒子を作製するためにはさらなる条件として，周囲に配するリポソーム粒子数が過剰であること，リポソーム粒子径が中心粒子径の1/3以下であることが望ましい。これにより異種粒子間の架橋反応による大きなフロック形成(図2(a))を抑えるのと，中心粒子に付着している周辺粒子間反発力を中心粒子との引力に比べ小さくすると共に配置構造的にも望ましい状況が実現される(図2(b)参照)。

さらに，複合微粒子の構造を安定化するためには異種粒子間に架橋を形成するとよい。電気二重層相互作用の引力による会合体(凝集体)は溶液の電解質濃度の変化で影響を受けやすいが，異種粒子間にバインダー(架橋分子)を用いることにより複合体構造を安定化することができる。高分子やタンパク質などはこの役目を担うものである。

2.2　リポソームを含む複合微粒子の作製例

2.2.1　シリカ／PCリポソーム系

中心にシリカ粒子，その周りにリポソーム粒子，さらにその周りにシリカ粒子を付着させた複合微粒子について述べる。塩化ランタン濃度10^{-4}Mの水溶液中で中心粒子となるシリカ粒子(粒子径1.5 μm)にPCリポソーム(粒子径200 nm)を付け，さらに0.5 μmのシリカ粒子をその上に付着させた系の写真を図3に示す。中心となるシリカ粒子分散液(塩化ランタン濃度10^{-4}M)にシリカ粒子数に比べ過剰粒子数のPCリポソーム分散液(塩化ランタン濃度10^{-4}M)を加え，2時間ほど撹拌し，金平糖型シリ

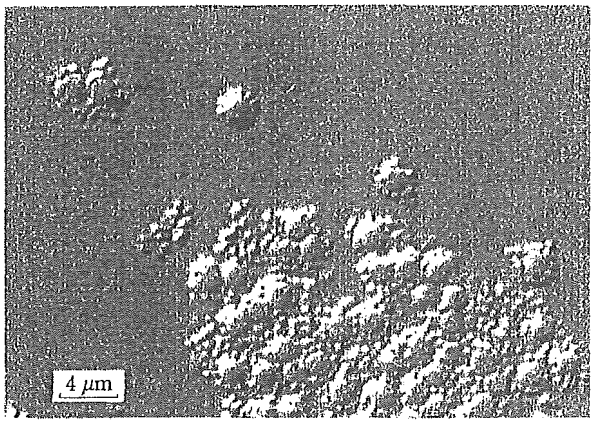

図3　シリカ／リポソーム／シリカ3層複合粒子の光学顕微鏡像

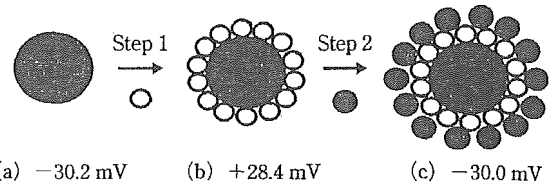

図4　シリカ／リポソーム／シリカ　3層構造形成過程における粒子表面電位(ゼータ電位)の変化

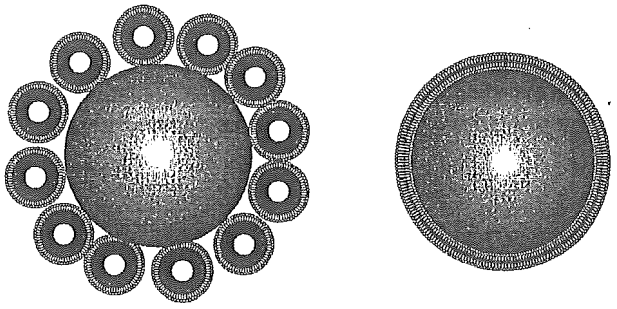

図5　中心粒子上の(a)リポソーム粒子単層吸着と(b)脂質二分子膜吸着の模式図

カ／PCリポソーム複合粒子を形成させる。過剰に残ったリポソームは遠心処理や限外ろ過などで取り除く。ここで使用するリポソームはリン脂質(PC, 卵黄ホスファチジルコリン：Sigma社から購入)から形成したものである。PCをエタノール溶液とし，窒素ガス風乾により試験管壁面に付着させた後，高速撹拌により純水に分散，その後フィルタリングやエクストルージョン法により約200 nmサイズまで粒子サイズを下げたものである。このように出来た複合微粒子分散液にさらに0.5 μmのシリカ粒子分散液(塩化ランタン濃度10^{-4}M)を粒子過剰量加え同様に撹拌処理と過剰粒子の分離処理を行うとシリカ／PCリポソーム／シリカの3層複合微粒子ができる[1]。作製過程の各段階で電気泳動測定を行うと粒子表面が負→正→負と変換されていることが分かる(図4参照)。これは複合粒子表面にある粒子種に対応している。きれいな3層構造になることから，2層構造においてもきれいな構造ができていることが分かる。シリカ粒子の表面に付いたリポソームがリポソーム状であるか，崩壊して二分子膜状になってしまっているかは(図5)，シリカ粒子上へのリン脂質の吸着量測定(リンの定量)や動的光散乱による粒子径の増加量を調べることにより判別できる。この場合はシリカ粒子表面上にリポソームの粒子が単層で吸着していることが示されている[2]。

2.2.2　磁性微粒子／PCリポソーム系(マグネト・リポソーム)

磁気微粒子の周囲にリポソーム粒子が付着した複合微粒子の作製について述べる。

磁性微粒子であるヘマタイトは酸化鉄の一種である。塩化鉄を原料に粒子径1 μm前後のヘマタイト微粒子を合成し中心粒子として使用する。まず，各種濃度の$FeCl_3$水溶液を密栓瓶中で100℃で各時間処理する[3]。粒子サイズは仕込みの塩化鉄濃度と反応時間で決まる。粒子径1 μm前後のヘマタイト微粒子分散液を選択し，粒子サイズを揃えるために沈降分離処理を数回～十数回繰り返す。ヘマタイトは超常磁性微粒子であるため磁気的相互作用による自己凝集が少なく，外的磁場がかからない限り単粒子として水中に分散する傾向にある。これは均一磁場により会合し線状構造をとる。また，勾配磁場を用いれば磁場強度の大きい所へ集めることができる。我々が作製したヘマタイト粒子は磁気泳動速度係数として約0.01(cm/s)(T/cm)程度のものである(Tは磁場強度テスラ)。さらに，ヘマタイト粒子の水中での単粒子としての分散性を上げるために，表面にシリカ層を合成する。この処理で負の表面電荷量を増加させ静電的反発力を増すと同時に水和反発力を加え非常によい単粒子状態で水中に分散させることができる(図6参照)。シリカ層合成はテトラエトキシシランを加水分解することで行う。表面がシリカでコーティングされた状況は粒子の電気泳動度測定

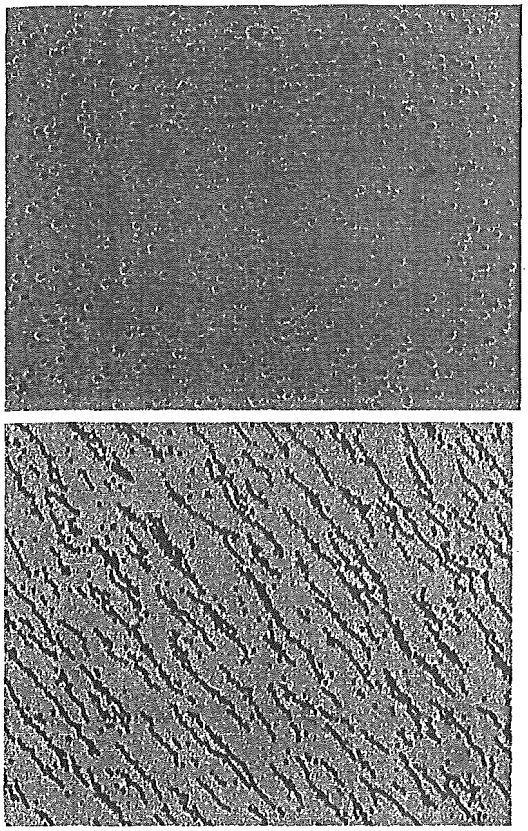

上：磁場がかかっていないとき。単粒子としてブラウン運動をしている。下：数百ガウス程度の磁場による磁気微粒子の集積と配向。線状会合体として蛇行運動している

図6　シリカをコートしたヘマタイト

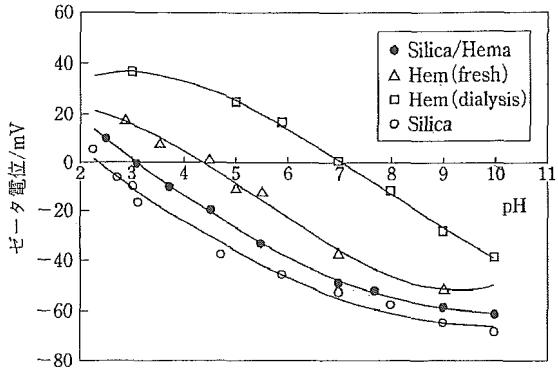

Hem(fresh)：合成直後のヘマタイト粒子，Hem(dialysis)：純水で長時間透析した後のヘマタイト，Silica：シリカ粒子，Silica/Hema：シリカ層を持つヘマタイト

図7　種々の粒子のゼータ電位のpH依存性

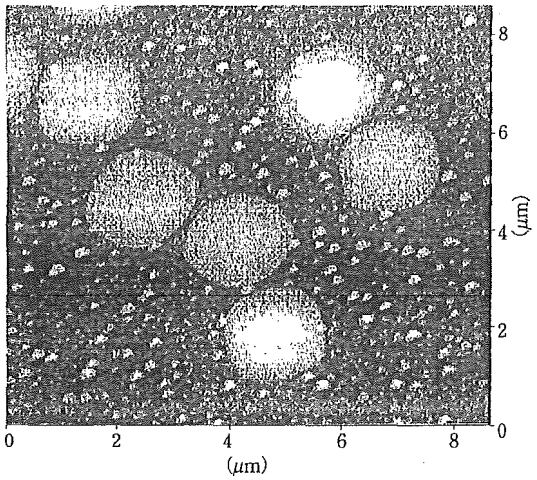

密着型X線透過像のPMMA樹脂のレプリカをAFMで読み出した像(産業技術総合研究所，眞島利和氏の撮影)

図8　シリカコートされたヘマタイト粒子のX線顕微鏡像(口絵参照)

により知ることができる。図7にヘマタイト粒子，シリカ粒子，シリカ層を持つヘマタイト粒子の表面電位(ゼータ電位)のpH依存性を示す。透析を繰り返した後の表面をきれいにしたシリカ層を持つヘマタイトはシリカ粒子とほぼ同じ等電点を示し，シリカコーティングが完成されていることが分かる。このシリカ層を表面に合成した粒子はpH中性領域では大きな負電荷を持ち，粒子間反発力を持つことが分かる。これは光学顕微鏡観察により非常によい単粒子状態で水中に分散することも確認される。また，X線顕微鏡(図8)や透過型電子顕微鏡により，シリカ層が滑らかにヘマタイト粒子表面に形成されていることについても確認できる。

この粒子表面上にさらにリポソーム粒子を付着させる方法としてはヘテロ凝集法やタンパク質を架橋分子としたブリッジング法を使う。タンパク質は種々の表面に物理吸着し，その過程は多くの場合不可逆吸着であることが知られている。タンパク質としてはpH中性領域で正味の正荷電を持つ塩基性タンパク質のcytochrome Cやlysozymeを用い，電気的相互作用と架橋効果を利用する。タンパク質濃度1 mg/mlの水溶液とシリカコートされた磁気微粒子を混合し，数時間吸着処理した後，タンパク質が吸着した微粒子を沈降させ上澄みをそのつど除去する。これを繰り返して得られた沈降粒子をタンパク質吸着微粒子試料とする。さらに，この試料粒子とリポソーム分散液と混合し，上記と同様な処理で金平糖型複合微粒子マグネット・リポソームが作製できる。作製プロセスを確認するため，各ステップで形

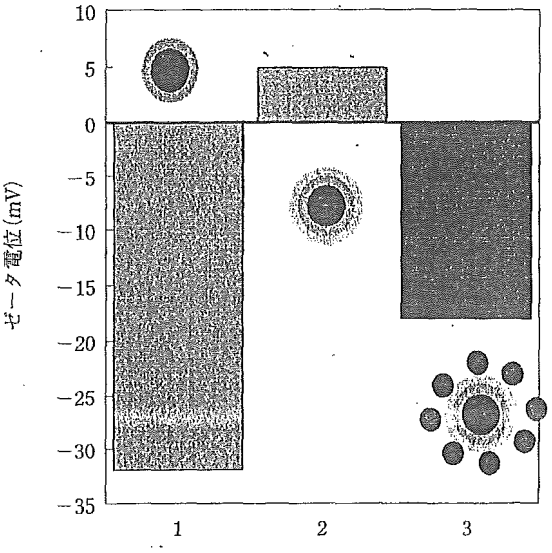

1：シリカコートされたヘマタイト，2：さらにリゾチーム吸着された粒子，3：さらにリポソームが吸着した複合粒子(マグネト・リポソーム)

図9　マグネト・リポソームの作製過程における各段階のゼータ電位

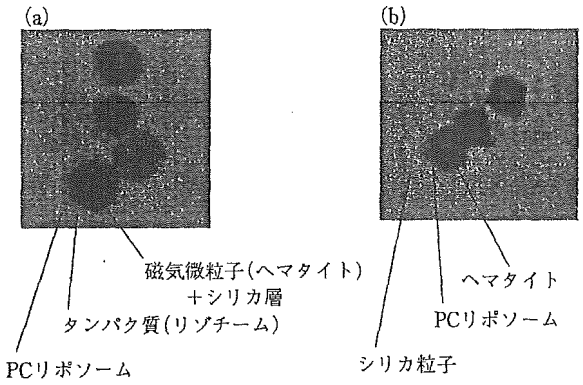

図10　(a)マグネト・リポソームの光学顕微鏡像
(b)シリカ粒子をさらに吸着させたもの

成される微粒子表面の電荷符合の測定を電気泳動測定法でしらべると，表面に付く分子や粒子の種類に対応して表面電荷(および表面電位)の正負が変わることが示され，目的のものが出来たことが確認される(**図9**参照)。光学顕微鏡観察を容易にするためにさらに0.4 μm程度のシリカ粒子を外側に付着させたものの像を**図10**に示す。

3. リポソームのエレクトロ・パーミエーション

細胞やリポソームに電場を印加すると，これらの膜の基本構造である脂質二分子膜の物質透過能が増加することが古くから知られている。これはエレクトロ・ポレーションとして細胞融合や遺伝子導入などの*in vitro*実験では今日広く使用される技術になっている。*in vivo*(臨床的)には先に述べたエレクトロ・ケモセラピーとして研究と臨床実験が展開されている。リポソームやリポソーム含有複合微粒子をエレクトロ・ケモセラピーに利用することを考えると，リポソームの膜透過能と印加電場との関係を明らかにすることが重要である。ここでは，Caイオンのリポソーム膜透過の電場依存性について紹介する。

3.1 Caイオンを内相に含むリポソームの作製

この実験に使用するリポソームの作製は以下のようである。リン脂質(卵黄ホスファチジルコリン：Sigma社)をエタノール溶液とし，窒素ガスを吹き付けて風乾しながら試験管を高速回転することにより試験管壁面に厚膜状態で付着させた後，Caイオン0.2 Mの水溶液を加え高速撹拌により分散する。その後，フィルターリングとエクストルージョン法(1 μmと0.2 μmポア径のメンブランフィルターを使用)によりサイジングし約0.2 μm粒子径のリポソームを得る。さらに−20℃←→＋40℃の温度履歴を2回施し，膜の分子パッキングを良くする。外相の溶液からCaイオンを取り除くため，透析チューブ(分画分子量10,000)を用い蒸留水に対して透析を4℃において5～6回繰り返す。こうして出来たリポソーム粒子径の確認は動的光散乱法で行う(粒子径は約200 nmのリポソームであることが確認される)。

リポソーム内相から外溶液中へのCaイオン流出の程度はCaに対する選択性蛍光分子(Quin 2)を用い両者の結合反応による蛍光強度増加で検出する(**図11**参照)。この場合外相溶液に蛍光分子Quin 2を含む溶液を用いる(この逆の組み合わせの試料系も実験可能)。蛍光測定は通常の蛍光分光光度計を用い励起波長は339 nm，観測波長は492 nmで行う。

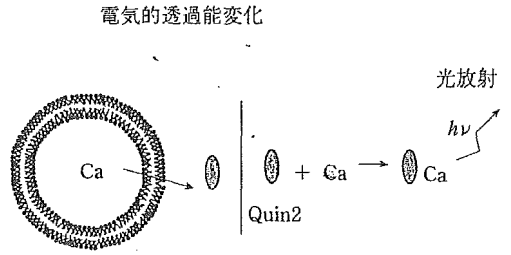

図11　Caイオン流出によるQuin 2との結合反応と蛍光

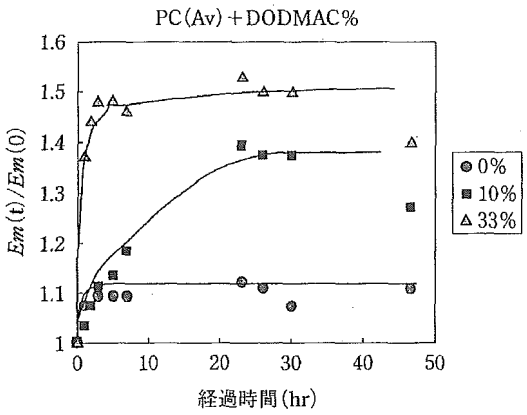

Caイオン流出による蛍光強度の増加の時間変化。%はカチオン性脂質分子の重量混合率

図12　リポソーム膜の安定性

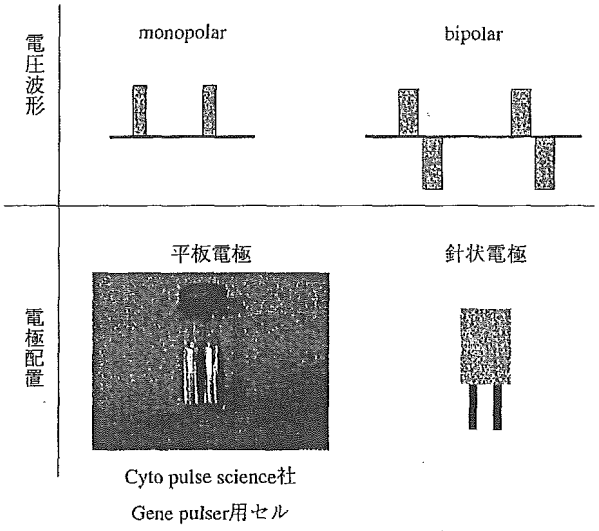

図13　電圧波形と電極形状の例

冷暗所(4℃)に放置保存したリポソーム試料の内相から流出してくるCaの量の経時変化を測定することによりリポソーム膜の安定性を評価する。PCのみのリポソームの場合はCaイオン保持能が高い。比較のためカチオン性脂質(ジオクタデシルジメチルアンモニウムクロライド)を混ぜたリポソームを作製しその安定性を調べると，Caイオン保持能は混合濃度と共に急激に下がる。二分子膜のパッキング状態が悪くなっている。図12に3種類のリポソームについての蛍光強度の径時変化の様子を示す。カチオン性脂質の混合がないものは長期安定性を持つが，混入量が増えるに従い蛍光強度が急激に増加し長期安定性に欠ける様子が見られる。

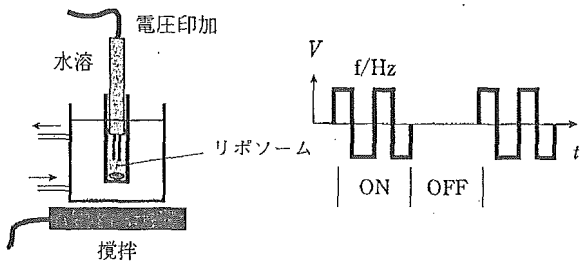

図14　この研究で使用した電極，セル，電場波形

3.2　電場印加

現在，エレクトロ・ケモセラピーでは針状電極や線状電極が使用されている。また，電場波形としてはmonopolar型パルス(米国Genetronics社等)とbipolar型(ブルガリア科学アカデミー，Daskalov教授)が使用されている(図13参照)。エレクトロ・パーミエーションに使用した我々の実験セットは以下のようである(図14参照)[4)5)]。電極構造と電場波形は針状電極，交流矩形波を使用する。ファンクションジェネレータで発生させた交流矩形波信号をバイポーラー型電圧・電流増幅器で増幅する。周波数は10～100 kHzを用い電場強度のピーク間電圧は最大140 Vで，これを1 mm間隔の白金線電極に加える。白金線の径は1 mmである。電場印加されるリポソーム分散サンプル量は約3 mlでマグネッチクスターラーにより常時撹拌すると共に水浴にて温度コントロールする(水浴温度は7℃)。試料溶液の温度上昇は電子温度計を投入して計る。

図15は典型的な蛍光強度の増加(Caイオンの流出量に対応)の電場周波数依存性である(ピーク間電圧：125 V，30秒印加，外液の電解質NaCl濃度0.02 M)。膜透過能の周波数依存性が1 kHzに極小を持ち両サイドで増加することを示す。これは低周波側での増加が電極による電気分解効果の結果起こるサンプル溶液の実効電気伝導度の増加によるもの(印加電圧を増加するにつれて100 Hz以下の電極を

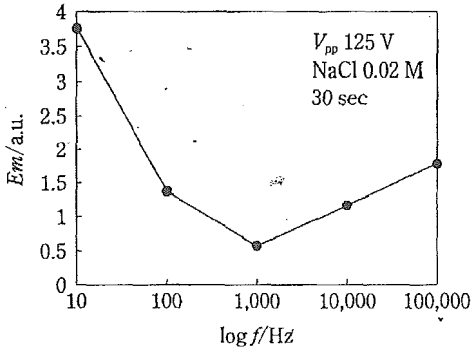

印加電圧125 V_{pp}，外液のNacl濃度0.02 M，印加時間30秒

図15　電場印加後の試料溶液の蛍光強度増加量の電場周波数依存性

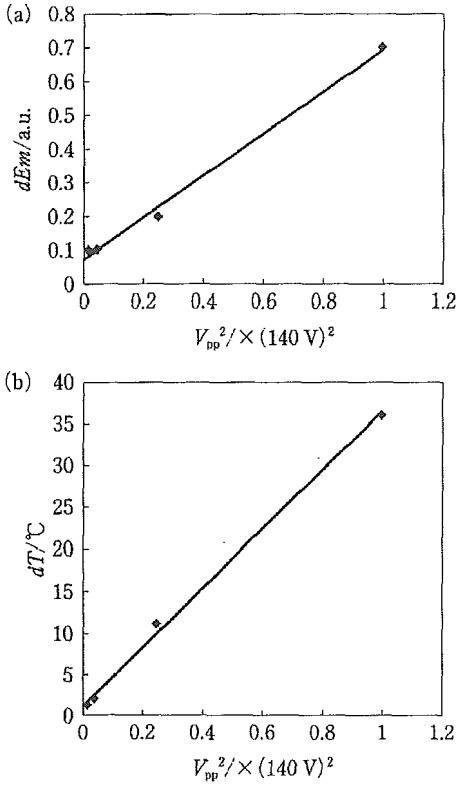

図16　蛍光強度増加(a)と温度増加(b)の電圧2乗依存性

含むセルインピーダンスは極端に減少することが示される)，また，高周波側での増加はコロイド分散系の実効電気伝導度の周波数依存性によるものであると解釈することができる(電気二重層を持つコロイド分散系の電気伝導度は粒子表面の電気伝導が大きな役割をはたし，この周波数領域では高周波になるほど増加する傾向にある)。実際この実験系ではサンプルの温度上昇が大きく，電気伝導度の上昇に

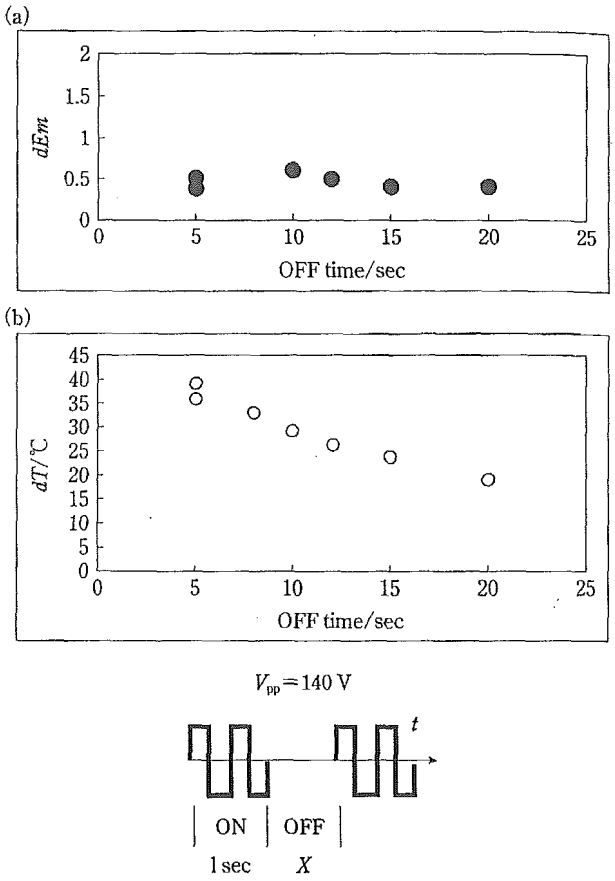

図17　蛍光強度増加(a)と温度増加(b)の電場印加間隔(X)に対する変化

より電気エネルギーが温度へと転換されていることが示される。

ところで，交流矩形波のturn onとturn offを繰り返すことで過剰な温度上昇は避けることができる。そこで，標準的な実験のプロトコルとして100 kHz矩形波で1秒間のON，5秒間のOFFの繰り返し7回を選択している(図14参照)。

先に述べた周波数依存性をサンプルによる電気エネルギー消費すなわち実効電気伝導度の変化によるとの解釈は膜透過能の電圧強度依存性とサンプル温度上昇のそれとを調べ比較することにより確認される。図16に示すように蛍光強度の変化分が電圧の2乗に比例すると同様に試料セル全体の温度上昇も電圧の2乗に比例することが分かる。これは電気エネルギーの消費が実効電気伝導度と電場強度の2乗の積で表される関係式に合致し，温度上昇は電気伝導度に起因するいわゆるジュール熱，同様に，蛍光強度上昇も電気伝導度増加に起因する膜透過能の変化と理解される。この系で使用された電場強度は

ピーク間125 V/1 mmすなわち，直流分としては62.5 V/1 mmであり，これは2分子膜間では約10 mV程度である。この大きさは，エレクトロ・ポレーションで使用されるパルス電場での有効強度(200～1,000 mV/膜間)より一桁も少ない。

一方，電場印加のturn off時間を変化させて同様な実験を行うと異なった結果が得られる。図**17**に蛍光強度変化と温度上昇のOFF時間依存性を示す。膜透過能すなわち蛍光強度の変化分はOFF時間を長くしても不変であるが，温度上昇はOFF時間が長くなるほど減少する傾向を示す。これは電場印加で発生する熱は，周囲への熱拡散が行える十分な時間間隔をとれば温度上昇を押さえることができ，同時に膜透過機能変化に十分効果を与えるプロトコルが存在するということを示している。すなわち，膜透過能はミクロな領域でのエネルギー消費と密接な関係にあることが示唆される。

【参考・引用文献】

1) B. Yang, H. Matsumura, K. Katoh, H. Kise and K. Furusawa : *Langmuir*, **17**, 2283–2286 (2001).
2) B. Yang, K. Furusawa and H. Matsumura : *Langmuir*, **19**, 9023–9027 (2003).
3) K. Furusawa, H. Matsumura and T. Majima : *J. Colloid Interface Sci.*, **264**, 95–100 (2003).
4) H. Matsumura, V. Neytchev, N. Terezova and I. Tsoneva : *Colloids & Surfaces B*, **33**, 243–249 (2004).
5) V. Neytchev, N. Terezova, H. Matsumura and T. Tomov : *Histol. Histopathol.*, **17**, 649–656 (2002).

<松村　英夫>

Colloidal Nanoparticles: Electrokinetic Characterization

Kunio Furusawa
University of Tsukuba, Ibaraki, Japan

Hideo Matsumura
National Institute of Advanced Industrial Science and Technology, Tsukuba, Japan

INTRODUCTION

A charged colloidal particle suspended in an electrolyte solution is surrounded by a cloud of counterions. The set of the surface charges and countercharges is called the electrical double layer. The electrical double layer plays an essential role in various interfacial electrical phenomena on the particle surface and in the particle–particle interaction of colloid suspension.

Generally, it is almost impossible to measure the surface potential on colloid particles. However, we can measure the potential near the particle surface. It is called the zeta (ζ) potential. The zeta potential is the potential at the hydrodynamic slipping plane in the electrical double layer, hence its value is not precisely the same as that of making a stable suspension because the total interaction potential between two particles a bit distant from their surface is essential for a stable dispersion. The ζ-potential has been considered to provide useful information necessary for preparing stable colloidal suspensions in many application fields including food preparation, agriculture, pharmaceuticals, paper industry, ceramics, paints, coatings, photographic emulsions, etc. The concept of the zeta potential is also very important in such diverse processes as environmental transport of nutrients, sol–gel synthesis, mineral recovery, waste water treatment, corrosion, and many more.

OVERVIEW

These are several origins from which solid surfaces are charged: dissociation of chemical groups on the surface, preferential adsorption of cation or anion onto the surface, etc. The distribution of each ionic compound between the surface and the solution bulk is determined by the differences in the electrochemical potential of each compound between two phases: the solid (surface) phase and the solution phase. Therefore the composition of the solution is an important factor that determines surface potentials. When H^+ is the potential-determining ion, we can change the amount of surface charge by changing the pH of the solution. It is important to know the position of the isoelectrical point (IEP) (i.e., the pH value at which the particles have zero ζ-potential). At the IEP, there are no repulsive forces and the particles are strongly aggregated because of the attractive van der Waals forces. In many cases, the stable colloidal particle dispersion is desired, so the colloidal suspensions are designed such that the pH of the suspension is well away from the IEP. The IEP data for a number of colloids of various compositions have been reported.[1] Table 1 lists the IEP for some typical dispersions.

If colloid particles are brought to a concentrated situation through some engineering processes, it is not certain if the surface charges, and hence surface potential, hold the same values as those in diluted dispersions. It must be measured experimentally, and several methods have been explored in recent years.

Here, we briefly describe experimental methods of the measurements of ζ-potential for the diluted and the concentrated particle systems, and how the control of zeta potential is useful for preparing composite particle systems in the last part of this report. The fundamentals of electrokinetics in colloidal systems have been described in numerous books in recent years.[1–3]

MEASUREMENTS OF ζ OF PARTICLES IN DILUTED SUSPENSION

Regular Method by Electrophoresis

The historical prominence of ζ-potential has been because of its experimental accessibility via measurement of the electrophoretic mobility μ. Electrophoretic mobility is the velocity of the colloid particle v per unit field strength E:

$$v = \mu E \tag{1}$$

Dekker Encyclopedia of Nanoscience and Nanotechnology
DOI: 10.1081/E-ENN 120009085

Table 1 *Isoelectric points*

Compound	IEP (pH)
α-AlOOH	9.4
γ-AlOOH	5.5–7.5
α-$Al(OH)_3$	5.0–5.2
γ-$Al(OH)_3$	9.3
CdO	10.4
Co_3O_4	5.5
$Co(OH)_2$	10.5
α-Fe_2O_3	8.3
βFe_2O_3	6.7–8.0
$Mg(OH)_2$	12
MnO, MnO_2	6
NiO	9.5
SiO_2	1.8–2.5
SnO_2	4.5
TiO_2	6
ZrO_2	4

where ζ is related with mobility by the equation from von Smoluchowski:[4]

$$\mu = \varepsilon\zeta/\eta \tag{2}$$

where ε or η are the permittivity or viscosity of the medium, respectively. In regular electrophoretic apparatus, we utilize a narrow capillary cell of cylindrical or rectangular shape. The migration velocity of the particles is measured by optical microscopy for larger-sized particles, or by observation of Doppler shift of laser light scattering signal for smaller particles. However, the capillary cell walls also bear electrical charges and hence have electrical double layers. Therefore the application of electrical fields causes the movement of charged liquid medium in the double layer, which is called electroosmosis. The electrophoretic migration of colloid particles is always superimposed on the electroosmotic liquid flow from the cell wall. The closed sample cell causes a back liquid flow through the generation of hydrostatic pressure gradient. At equilibrium, there are two positions where the liquid flow has zero velocity. These are called the stationary levels. Thus we can observe the true electromigration velocity of colloid particles at the stationary levels. Von Smoluchowski[4] showed the profile of electroosmotic flow velocity (U_{osm}) for a cylindrical cell:

$$U_{osm} = U_0(h^2/b^2 - 1) \tag{3}$$

and for a flat cell, which has an infinitely long width:

$$U_{osm} = U_0/2(3h^2/b^2 - 1) \tag{4}$$

where h is the distance from the cell center in the direction of cell thickness, b is the half-thickness of the cell, and U_0 is the electroosmotic flow at the cell wall ($h=b$). The stationary levels are located at a distance from the cell center to each side by the quantity $h=b/\sqrt{2}$ for the cylindrical cell, or $h=b/\sqrt{3}$ for the flat cell. Komagata[5] showed a more practically useful equation for a rectangular cell, which has a thickness of $2b$ and a width of $2w$ ($b<w$); the stationary level is located at a distance from the cell center to each side by the quantity $h=b\sqrt{(1/3(1 + 384b/\pi^5 w))}$. The traditional measurements of zeta potentials of particles are conducted at these stationary levels.

Electrophoretic Measurements Using a Standard Sample

The profile of electroosmotic flow is parabolical. Thus the velocity gradient of the liquid at the stationary levels is usually large and the observed velocity of the particles changes rapidly with cell depth. It causes substantial errors in electrophoretic mobility measurements from the wrong setting of observing points. However, if the electrophoretic measurements can be carried out by using a reference sample as a standard, the electrophoretic mobility of the unknown sample can be determined at any cell depth by subtracting the mobility of the reference particles at the same level, because the velocity of electroosmotic liquid flow induced by the cell wall has the same value under the same experimental conditions. Therefore one can obtain real electrophoretic mobility rather accurately by measuring the velocity at the cell center, where the velocity gradient is zero.

The apparent electrophoretic mobility (U_{app}) of an unknown colloid sample is always the sum of two contributions, one of which is the real electrophoretic mobility (U_{el}) and the other is the liquid flow velocity induced by the electroosmotic effect (U_{osm}) of the cell wall, which changes as a parabolical function of the cell depth:

$$U_{app} = U_{el} + U_{osm} \tag{5}$$

Similarly, the apparent velocity of the reference sample (U_{app}') was also indicated by the sum of the real electrophoretic mobility (U_{el}') and the electroosmotic flow velocity (U_{osm}'), that is,

$$U'_{app} = U'_{el} + U'_{osm} \tag{6}$$

Under the same experimental conditions, using a finite electrophoretic cell ($U_{osm}=U_{osm}'$), the following relationship holds from Eqs. 5 and 6:

$$U_{el} - U'_{el} = U_{app} - U'_{app} \tag{7}$$

If U_{el}' is known exactly, the U_{el} value of the unknown sample can be determined from the difference between

the two apparent mobilities at any cell depth. Thus if the particle mobilities of unknown samples and the reference sample are measured at the cell center where the migration velocity has a maximum, the real electrophoretic mobility of the unknown sample is given by:

$$U_{el} - U'_{el} = U_{app}(\text{maximum}) - U'_{app}(\text{maximum}) \quad (8)$$

Fig. 1 shows an example indicating the electrophoretic mobility profiles obtained experimentally for the reference sample (PSSNa lattices) and an unknown sample (SM lattices) along the cell depth in a 1×10^{-3} M KCl solution at 25°C. The SM lattices employed as an unknown sample were prepared by the copolymerization of styrene with 5% methacrylic acid (MA) at 70°C. It is apparent that both profiles indicate reasonable parabolical curves, and the curve for the reference lattices shows a constant mobility at the two stationary levels. Furthermore, the difference between the two apparent mobilities at the cell center agrees well with the velocity of the SM lattices at the stationary level.

Fig. 2 shows the ζ-potential vs. pH curves for the SM lattices, which have been determined from the maximum mobilities using the PSSNa lattices as a standard.[6] The same relation obtained from the velocity of the SM lattices at the stationary level is also indicated. As can be seen, both curves agree fairly well over the whole pH range. All of these results indicate that if we have a reliable colloid sample whose ζ-potential is exactly determined, the ζ-potential of the unknown sample can be determined precisely from the measurements of apparent electrophoretic mobility at the cell center. In that case, slight errors in focusing (i.e., errors because of the view field) are less important because the velocity gradient near the level of observation is very small.

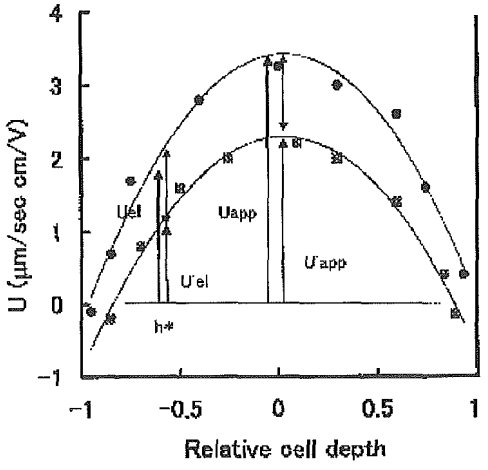

Fig. 1 Examples of electrophoretic mobility profiles of PSSNa lattices (U') and SM lattices (U). (h^*) stationary level; (■) PSSNa lattices; (●) SM lattices (1×10^{-3} M KCl, 25°C).

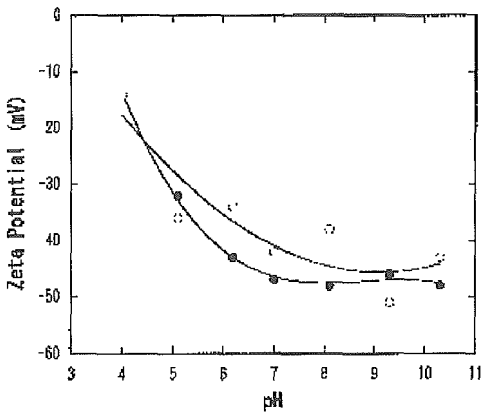

Fig. 2 ζ-Potential vs. pH curves of unknown sample (SM lattices) determined by the maximum velocity of reference sample (●) and the usual method (○).

According to Eqs. 3 and 4, U_0 and hence the ζ-potential of the cell wall are determined using a reference sample. The electroosmotic velocity (U_0) obtained by the extrapolation of the velocity profile to the cell wall permits the determination of the ζ-potential of the cell wall–solution interface, and the ζ-potential measurement of various solid–solution interfaces,[7] including the dissimilar cell system,[8] has been determined. Here, we would like to emphasize again that the determination of the ζ-potential of the cell wall is also possible from the maximum velocity of the reference sample, instead of the tedious plane interface procedure. According to Eq. 4, the apparent velocity of the reference sample at the cell center (at h=0) is $U_{app}' = U_{el}' - U_0'/2$. Therefore U_0' and hence the ζ-potential of the cell wall can be quickly determined if the U_{el}' has been previously known.

Fig. 3 shows some examples of apparent flow velocity profiles of standard latex samples (PSSNa lattices) at various pH values in which both boundaries refer to the glass–solution interface. A symmetrical parabola was given at all pH conditions where the surface charge of glass is consistent with both sides.

ELECTROKINETIC CHARACTERIZATIONS IN CONCENTRATED DISPERSIONS

In recent years, electroacoustics offered studies on surface characterization and the stability of suspended colloid particles. The term electroacoustics refer to two kinds of related phenomena: 1) colloid vibration potential (CVP),

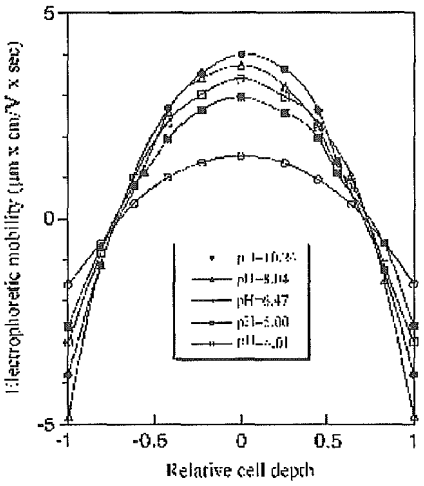

Fig. 3 Apparent flow velocity profile of standard latex samples at various pH values (1×10^{-3} M KCl, 25°C).

in which an electrical field arises in colloidal suspension when a sound wave passes through the dispersion (i.e., ultrasonic vibration causes the difference in movement between charged core particles and countercharges around them, which induces oscillating dipole moments and hence the potential drop in the sample cell);[9] and 2) electrokinetic sonic amplitude (ESA), the reciprocal effect of the above phenomena, in which an alternating electrical field is applied to a suspension and a sound wave arises as a result of the inertia of the particles, caused by their time-alternating electrophoresis (i.e., high-frequency electrical waves cause a difference in movement between the core particles and the countercharges, which generates an ultrasonic waves in the sample cell).[10,11]

A very important advantage of these electroacoustical techniques is their ability to provide accurate measurements of the ζ-potential in concentrated colloid systems. In this section, two of the typical data obtained by these methods are shown.

Surface Characterization of Concentrated Latex Suspensions

In this section, the CVP technique is demonstrated for zeta potential measurements of concentrated suspensions of latex particles with different surface groups.[12] Three types of polystyrene lattices with different surface groups were synthesized in emulsifier-free systems. The usual polystyrene (PSt) lattices were prepared by the method of Kotera et al.,[13] and the two others (PSm and PStn) were synthesized by incorporating small amounts of ionic

Table 2 Characterization of colloid particles

Sample	Diameter (nm)	Surface charge density (μC/cm²) Strong acid	Weak acid	Total
PSt	480	5.3	2.5	7.8
PStn	610	18	0	18
PStm	530	5	33	38

comonomer, methacrylic acid, and sodium polyvinylphenylsulfonate (NaSS) into a polystyrene chain, respectively, as in Juang and Krieger.[14] To increase the particle size, PStn was prepared in a system with 1×10^{-4} mol/dm³ $MgSO_4$. These latex samples were sufficiently dialyzed with distilled water and were then brought into contact with an ion exchange resin to remove ionic impurities. The samples were all composed of highly monodispersed spherical particles with $D_w/D_n=1.02$, and the surface charge densities of the latex particles were measured by potentiometric and conductometric titration, as in Van den Hul and Vanderhoff.[15] The characterization data of all the samples are summarized in Table 2.

To compare the CVP with the conventional electrokinetic technique, first, the zeta potential of each sample in a dilute state was determined in a 1×10^{-3} mol/dm³ KCl solution at different pH values using the microelectrophoretic technique. The resulting data for four samples are shown in Fig. 4. The ζ-potential of the latex samples, especially the PStn sample, appears to be essentially independent of the medium pH. The zeta potential of PSt increases gradually from acidic to neutral pH. This behavior is probably dependent on the existence of carboxyl groups on the surface (with pK_a values between

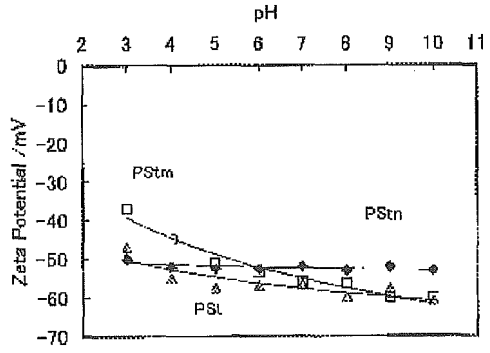

Fig. 4 pH dependence of zeta potential in dilute state measured by the microelectrophoretic technique in 1×10^{-3} mol/dm³ KCl at 25°C.

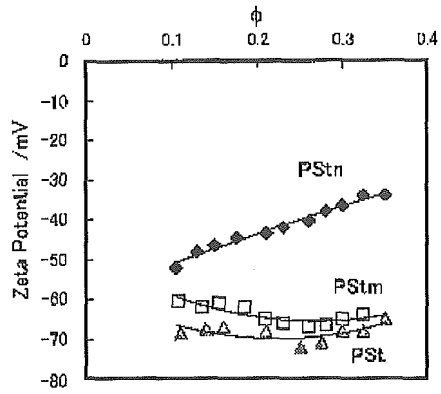

Fig. 5 Concentration dependence of zeta potential for polystyrene latex suspensions in 1×10^{-3} mol/dm^3 KCl at 25°C and pH 5.

about 4 and 5), which are produced by the hydrolysis and subsequent oxidation of the OSO_3^- groups that come from the radical fragments used as an initiator ($K_2S_2O_8$).[16–18]

The CVP measurements of polystyrene lattices give reliable data only in high-volume fraction (ϕ) systems above $\phi=0.1$ because the density of the latex particles is small ($\rho_2=1.05$ g/cm^3) and significant differences of CVP against the background signal can be detected only at high concentration ranges. Figs. 5 and 6 are graphs of the zeta potentials determined by CVP measurements for three kinds of polystyrene lattices at pH 5 and 9, as a function of the ϕ value of each latex. It is apparent that the zeta potentials for PSt and PStm at pH 5 and for PSt at pH 9 have nearly constant values over the entire concentration range of particles, and that the cell model theory is nearly

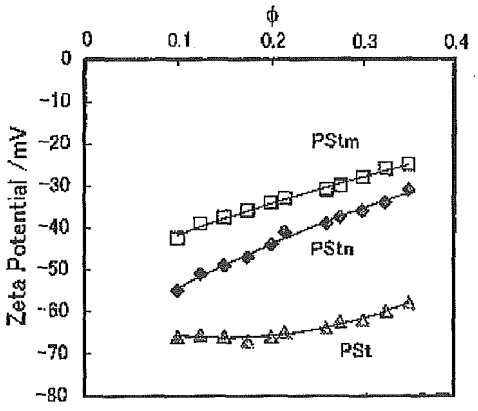

Fig. 6 Concentration dependence of zeta potential for polystyrene latex suspensions in 1×10^{-3} mol/dm^3 KCl at 25°C and pH 9.

valid for those systems. However, the zeta potentials for PStn at pH 5 and for PStn and PStm at both pH values decrease strongly as the particle concentrations increase. Furthermore, it was found that those of PStm at pH 9 are lower than those at pH 5, which is opposite in tendency to those in Fig. 4, determined directly in dilute states by the microelectrophoretic technique. It is thought, from a comparison with Table 2, that this abnormal behavior of the ζ-potential is related to the high surface charge densities of the latex samples (i.e., PStn has many sulfonate groups on the surface brought about by the NaSS component), which dissociate completely under both pH conditions, and PStm becomes covered with thick carboxyl layers coming from the MA molecules, which gradually dissociate as the pH increases. These high surface charge densities bring about an expansion of the surface layer and may cause a double-layer overlapping at moderate particle concentrations, which results in restrictions for the prerequisite of the cell model of Levine et al.[19]

To understand the abnormal behavior of the CVP and ζ-potential that appeared in the latex suspensions, including the particles with high surface charge densities, the concentration dependence of conductivity was measured in the respective systems. The concentration dependence of the conductivity depends largely on the surface nature of the particles.[12] The conductivity of polystyrene latex systems increases as the particle concentration increases. This tendency is especially remarkable in the PStn systems at pH 5 and 9 and in the PStm system at pH 9. From a comparison with the results of the CVP, it was realized that this increasing tendency of the conductivity is closely related to the abnormal behavior of the CVP. This is explained as follows. On the highly charged surfaces of PStn or PStm at pH 9, a polyelectrolyte-like (''hairy'') layer is present. These layers overlap each other in this concentrated state, allowing electrical conduction through the hairy layer; thus the hairy layer results in interparticle surface conductance. The degree of interparticle surface conduction is affected by the particle concentration and the thickness of the hairy layer, which in turn depend on the surface charge density of the particle and the pH of the medium.

Application of Electrokinetic Sonic Amplitude Technique in the Ceramic Industry

The concept of colloidal suspension processing has been successfully applied to the field of structural ceramic where inherent properties of dense suspension are used to transform a fluid suspension to a stiff gel. During colloidal processing, the state of dispersion has a significant influence on the casting behavior and the resulting green body properties. The good dispersion of particles

gives optimum packing state (high green density), which influences the sinterability of the ceramic body and hence the physical and chemical properties of the final product. At present, fine-grained and uniform microstructures are desirable for most ceramic applications in producing strong and reliable structural parts.

Traditionally in the ceramic industry, polyelectrolytes have been utilized to prevent the flocculation of particles. Because of the charged nature of the polyelectrolyte, they impart stability to the particles via an electrosteric mechanism. Hence the adsorption of these charged molecules onto a particle surface will alter the surface charge and hence the zeta potential. Thus using electroacoustics, it is possible to follow the changes in the zeta potential with increasing amounts of polyelectrolyte. This is extremely useful in determining the optimum amount of polyelectrolyte required to stabilize the particles under different conditions.

Fig. 7 shows how the zeta potential of an alumina suspension (background electrolyte, 10 mM KCl) can be altered by the addition of three commercially available polyelectrolytes.[20] Initially, the zeta potential of the suspension is such that the suspension becomes more stable. The trend for all dispersants is very similar in that, initially, the zeta potential changes strongly with small amounts of dispersants and then after a certain concentration, the zeta potential begins to plateau out as no more dispersant is adsorbed on the surface. However, each dispersant imparts a different final zeta potential and requires a different amount of dispersants to cover the particles. Of these, Poly-CA imparts the greatest final zeta potential, so this would be an excellent dispersant for the alumina. However, it must be noted that the likely stabilization mechanism for polyelectrolyte dispersants is electrosteric stabilization. Therefore there may well be a steric contribution to the stabilization mechanism depending on how the dispersant adsorbs. Poly-CE64 imparts a final zeta potential of -45 mV and requires approximately twice as much dispersant to do so, making it a poor candidate in comparison. The zeta potential from the suspension stabilized with Poly-PC 33 does not appear to level out, and further data points would be required to determine the optimum amount.

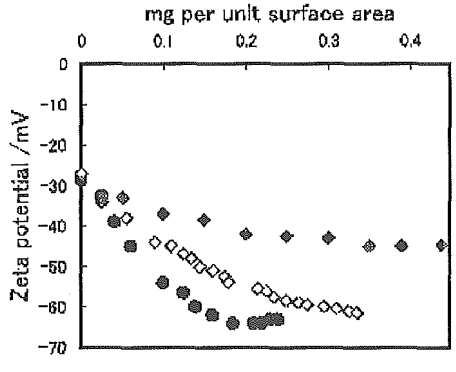

Fig. 7 Effect of three commercial dispersants on alumina suspension in 1×10^{-4} mol/dm^3 KCl: (●) Poly-CA; (◇) Poly-PC33; (◆) Poly-CE64.

ELECTROKINETIC MEASUREMENTS IN SYNTHESIS OF COMPOSITE PARTICLES

There is a variety of methods currently used to fabricate a wide range of stable, composite, and coating particles of various compositions. These include heterocoagulation,[21] seed polymerization,[22] emulsion/phase separation,[23] sacrificial core techniques,[24] and so on. The notion of adsorbing particles onto solid substrates in a layer-by-layer manner was introduced by Iler[25] in the mid-1960s. Decher and Hong[26] extended Iler's work to a combination of linear polycations and polyanions in the early 1990s. Decher[27] later adapted the layer-by-layer technique to include inorganic nanoparticles, biomolecules, clays, and dyes in polyelectrolyte multilayer assemblies. Very recently, Caruso and Mohwald[28] and Caruso et al.[29] reported very interesting results, which included a detailed investigation of the stepwise formation of the silica–nanoparticle/polymer multilayer templating of some latex particles. In this chapter, we demonstrate how we can utilize electrophoretic measurements in synthesis and coating processes of composite particles.

Heterocoagulation Behavior of Polymer Lattices with Spherical Silica

Gherardi and Matijevic[30] have investigated various behaviors of mixed colloid particles obtained by mixing differently preformed particles. They showed that the nature of a mixing system depends on the conditions of preparations, and concluded that the most important parameter in controlling the morphology of composite particles is the surface charge of the component particles, especially the contrast between surface charges of the two component particles. A stable system consisting of a regular composite particle could be prepared only in a medium controlled at a definite pH, where the two components are charged with opposite signs. Typical results

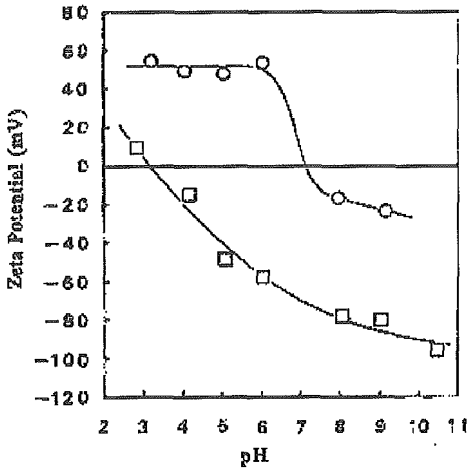

Fig. 8 ζ-Potentials of silica (□) and latex particles (○) as a function of pH at 5×10^{-3} mol/dm^3 KCl.

of the electrophoretic mobility for the single silica and the latex suspension are shown in Fig. 8.

The next important parameter to control morphology is the particle size ratio of the component particles when they are mixed in the vessel. Fig. 9 shows schematic pictures of the morphology of heterocoagulates of different silica particles and amphoteric lattices. Fig. 10 shows an optical micrograph of the real heterocoagulate generated from different silica samples and amphoteric latex systems, where the other conditions (e.g., the particle number ratio, $N_{silica}/N_{latex}=1/300$; medium pH 5.6) have been kept constant. The microscope used for

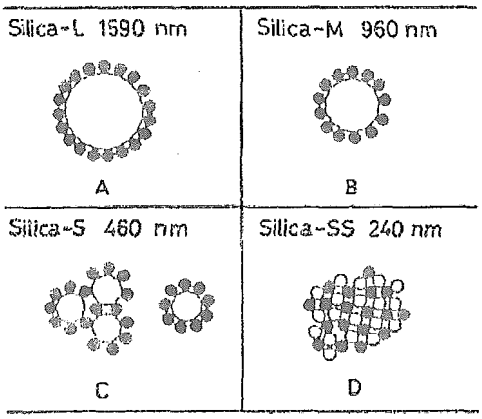

Fig. 9 Schematic pictures showing the morphology of heterocoagulate particles formed from different silica samples.

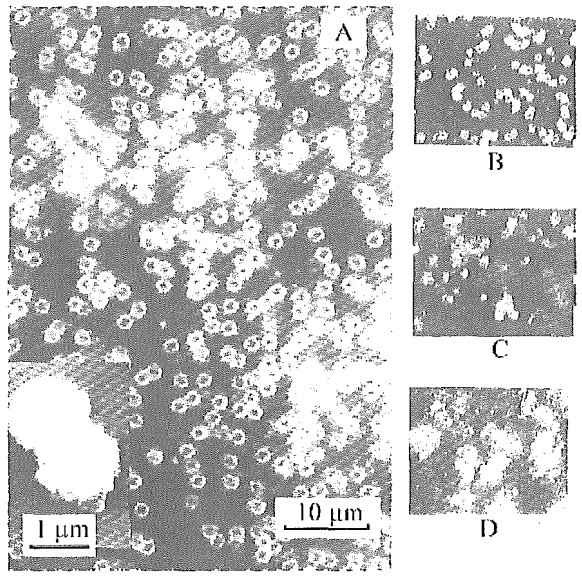

Fig. 10 Optical micrograph showing the heterocoagulates prepared from different silica samples: (A) Silica-L; (B) Silica-M; (C) Silica-S: (D) Silica-SS.

observations was a lateral-type metallurgical microscope (Axio Mart, Carl Zeiss, Germany). It may be seen that at a particle size ratio ($r=D_{silica}/D_{latex}$) higher than 3, the suspension is composed of uniform heterocoagulate particles and each heterocoagulate undergoes Brownian motion as an isolated unit. The insert of Fig. 10A shows a scanning electron micrograph of the heterocoagulate. It

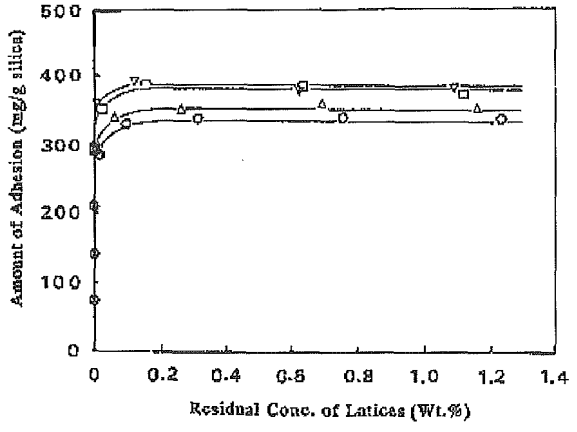

Fig. 11 Adhesion isotherms of amphoteric lattices onto Silica-L at various K_2SO_4 concentrations: (▽) 1.46×10^{-2} M; (□) 1.46×10^{-3} M; (△) 1.46×10^{-4} M; (○) 0 M.

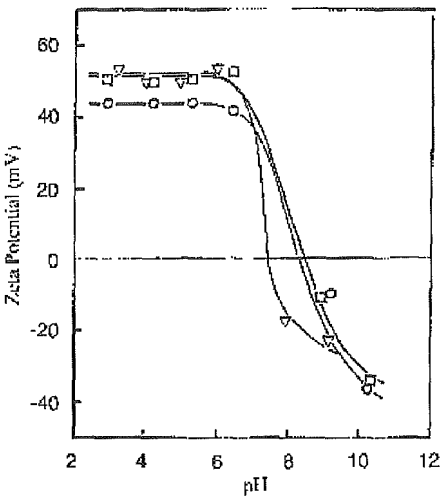

Fig. 12 ζ-Potentials vs. pH curves for heterocoagulate particles prepared at different electrolytes: (▽) heterocoagulates prepared at 2.48×10^{-1} M $MgCl_2$; (○) heterocoagulates prepared at 1×10^{-5} M KCl; (□) amphoteric lattices.

is apparent that the heterocoagulate takes a raspberry shape with one silica particle in the core. In contrast to this, the heterocoagulates generated at a particle size ratio lower than $r=3$ (Fig. 10C and D) are composed of large, irregular aggregates, and regular coagulates were hardly formed at any medium pH and particle number ratio investigated.[31,32]

It is interesting to analyze the different heterocoagulation behaviors from the concept of the adhesion isotherm for the amphoteric lattices on the silica particles. Fig. 11 shows some typical isotherms for the lattices on Silica-L at various K_2SO_4 concentrations, where all the systems were controlled at pH 5.2. It is evident that the isotherms are all well defined and of very high affinity type, and the plateau value increases with increasing K_2SO_4 concentration within the range from 10^{-5} to 10^{-2} mol/dm^3. This means that in this concentration range, adhesion proceeds in a way characteristic of monolayer adhesion. This may be because of the strong blocking effect of adhering particles. However, in K_2SO_4 aqueous solutions more concentrated than 2×10^{-2} mol/dm^3, no reproducible isotherm could be obtained under any conditions tested, and only some irregular aggregates were generated in the course of the experiment.[31] In Fig. 12, the ζ-potentials of the heterocoagulates prepared at different electrolyte concentrations, as well as the data on the amphoteric lattices, are presented as a function of the medium pH. As may be seen, a reversal of charge is observed in all samples, and the IEP in the heterocoagulated systems

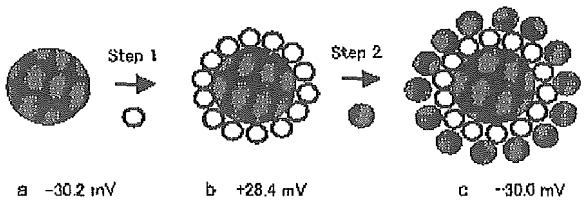

Fig. 13 Schematic showing the process of synthesizing multilayer composite particles: (a) core silica; (b) PC vesicle/silica composite particle; (c) silica/PC vesicle/silica composite particle.

occurs at about pH 8, which is not so different from the IEP of the single lattices. Moreover, the fact that the limiting net positive ζ-potential attained at $3 < pH < 6$ increases with increasing electrolyte concentration is also in line with the increase in latex adhesion with increasing electrolyte concentration.

Multilayer Composite Particles Comprising Silica/Vesicle/Silica Particles

Composite particles, including vesicle particles, are an important topic in application fields. Composite particles can be used frequently in the biomedical field for diagnostic purposes and for treatment medicine. Here, we describe one example of such systems,[33] that is, PC vesicles, which are typical biocolloid systems and are introduced into composites as a one-component particle.

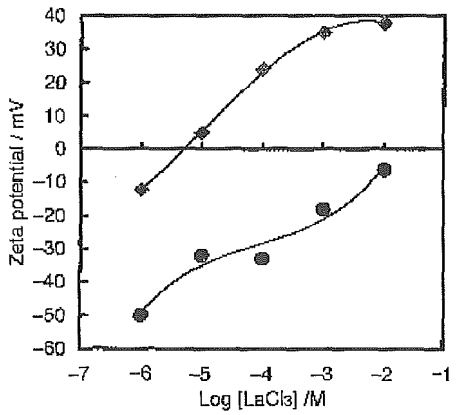

Fig. 14 ζ-Potentials vs. the concentration of $LaCl_3$: (◆) PC vesicles; (●) silica particles.

The silica/PC vesicle/silica multilayer composite particles were prepared by the alternate adsorption of PC vesicles and small silica particles on the large silica particles with negative charges (Fig. 13). In this study, electrostatic attraction is taken into account as the driving force. It is important that the silica and the vesicle surfaces bear opposite charges to be effective. We can control the surface charges of the vesicle and silica particles by adjusting the concentration of $LaCl_3$. In Fig. 14, the ζ-potentials of PC vesicles and silica particles are shown as a function of $LaCl_3$ concentration. The ζ-potential of PC vesicles decreases with increasing $LaCl_3$ concentration, and becomes positive over a certain concentration of $LaCl_3$. This is because of the binding effect of La^{3+} ions to the phospholipids head group.[34] However, for silica dispersions, the ζ-potential remained negative over the 10^{-6}–10^{-2} M concentration range of $LaCl_3$. Thus at 10^{-4} M $LaCl_3$, the ζ-potentials of the silica and PC vesicles were -30 and $+32$ mV, respectively. It is assumed that a strong electrostatic attraction will occur between the vesicles and the silica particles. Therefore we selected 10^{-4} M $LaCl_3$ as the heterocoagulation condition.

After mixing the PC vesicles with the core silica dispersion, the free vesicles were removed from the dispersion and the ζ-potentials of the composite particles generated were measured. The value was determined to be +28 mV. The positive ζ-potential indicates that the PC vesicles are adsorbed on the silica surface because the surface of the PC vesicles binds with La^{3+} ions.

For the PC vesicle adsorption state on the silica surface, there are two possible states: 1) as a vesicle particle layer, or 2) as a lipid molecular bilayer. To clarify the adsorption state of the vesicles, as the next stage, the adsorption amounts of PC on the silica surface have been measured. In Fig. 15, the results are shown as a function of the PC concentration. Adsorption amounts are expressed by the number of phospholipids molecules ad-

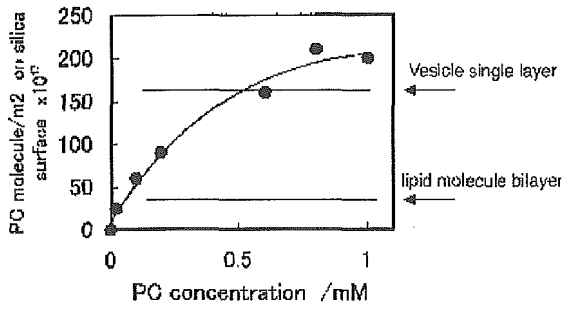

Fig. 15 Adsorption amount for PC on core silica surface in 10^{-4} M $LaCl_3$ at 25°C.

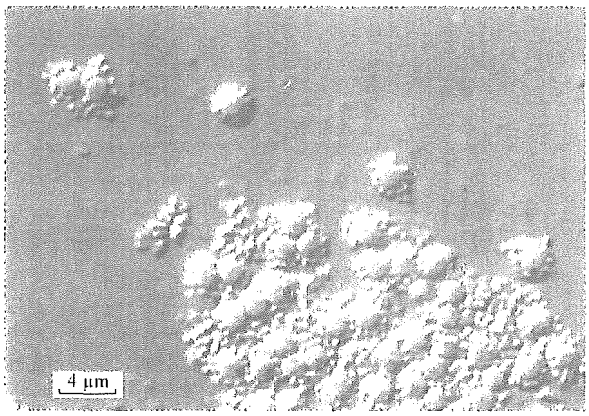

Fig. 16 Optical micrograph of silica/PC vesicles/silica composite particles. (*View this art in color at www.dekker.com.*)

sorbed per square meter of silica surface. The solid line represents a theoretical curve for the adsorption amount of the single bilayer model, assuming the area per PC molecule equals 0.7 nm^2. The dotted line shows a theoretical curve for the adsorption of a single vesicle layer model, assuming that the vesicles are of uniform size and have a unilamellar spherical shape. The saturated adsorption amounts in the experiments are located near the value for the latter, but over it. This is because of the existence of some multilamellar PC vesicles in the sample (i.e., the existence of multilamellar PC vesicles will induce a large number of PC molecules than the value of unilamellar vesicles). Thus we can expect that the PC vesicles will be adsorbed on the silica surface as a unilamellar vesicle layer (i.e., the composite particles have been generated as shown in Fig. 13b). Furthermore, we then separated the PC vesicle/silica composites from the free PC vesicles by the ultra-filtration method (with a polycarbonate membrane filter, pore size 1.0 μm), and determined the mean size of the composite particles by the dynamic light scattering (DLS) method. The diameter of the composite particles is 1.93 μm, and this value is close to 1.9 μm, which was calculated by the single particle layer model. This result means that the PV vesicles will be adsorbed on silica particles as the same spherical particle size.

In the second stage of composite formation, we mixed the PC vesicle/silica composite particles with a small silica ($2a$=0.5 μm) dispersion under the same 10^{-4} M $LaCl_3$ solution. The ζ-potentials of the products reversed from positive (+28.4 mV) to negative (-30 mV) again, which indicates that the small silica particles (with negative charges) were adsorbed on the surface of the positively charged composite particles (Fig. 13c).

The direct observation of the multilayer formation of composite particles is provided by a special optical microscopy technique. In Fig. 16, the composite particles of the silica/PC vesicle/core silica in the 10^{-4} M $LaCl_3$ solution are shown. We cannot clearly see the image of the PC vesicles on the silica because the PC vesicle has a large water core and a thin lipid bilayer (about 5 nm). Therefore the total refractive indices of the PC vesicle are close to those of water. However, the formation of the silica/PC vesicle/silica composite particles is indicated clearly in Fig. 16; the small silica particles are adsorbed on the spherical surface of the PC vesicle/core silica composite and are located on the outer layer of the composite particles.

The Buildup of Polyelectrolyte and/or Colloid Particle Multilayer on Solid Surfaces

The multilayer formation of polyelectrolytes on colloid particles is usually characterized by a stepwise increase of the adsorbed amount and layer thickness, and by alternating highly positive and negative ζ-potentials of the covered particles. Here, we describe two kinds of multicomponent layer systems using polyelectrolyte and colloid particles. One is the formation of polyelectrolyte multilayers on polymer colloids. Another is the formation of composite particles including organic and inorganic colloid particles using a layer-by-layer technique of polyelectrolytes.[35]

To emphasize the influence of the polarity of the substrate, three kinds of polystyrene lattices are employed. PS-740 lattices with large size ($2a$=740 nm) were prepared by the usual surfactant-free emulsion polymerization technique;[12] NaSS-190 lattices were made by incorporating a small amount of an ionic comonomer, sodium-*p*-vinylbenzyl-sulfate, into the polystyrene chain according to Kotera et al.[13] The charge density of NaSS-190 lattices is much higher than that of PS-740 latex. DEAM-250 lattices consist of amphoteric particles prepared by the method described by Homola and James.[36] Characteristic data for these samples are shown in Table 3. Silica samples with different particle sizes ($2a$=500, 300, and 20 nm), which were obtained from Nippon Catalisitic Co. Ltd. and Nissan Chemical Co. Ltd., were used. All these single dispersions consisted of monodisperse spherical particles with $D_w/D_n < 1.04$ always, and were used after extensive dialysis.

As the cationic polymer, poly-L-lysine (PLL-19) with a fixed molecular weight (M=190,000) was used, and as the anionic polymer, polystyrene sulfonate (PSSNa-50) with M=500,000 was used. PSSNa-50 carries a constant charge for pH 3–10. However, PLL-19 is pH-dependently charged and it is known that a fixed positive charge is carried only in the region of pH 3–7.

The adsorption of polyelectrolytes was allowed to take place for 1.5–2 hr at a 0.1–0.3 mg/mL PLL or PSSNa solution using a very dilute latex or silica suspension (ϕ=0.0001) and a saturated concentration without any free polymer of each polyelectrolyte that was determined by mobility measurements of the core particles. During the adsorption process, suspensions of the core particles were mixed slowly by means of rotating end-over-end.

The DLS measurements were carried out to assess the development of hydrodynamic layer thickness on the addition of PLL or PSSNa molecules. The heterocoagulated state of composite particles was observed directly by the optical microscope and scanning electron microscope.

Multilayer formation of polyelectrolytes on colloid particles

In Fig. 17, a typical cyclical curve of ζ-potential on alternating additions of PLL-19 and PSSNa-50 on negatively charged NaSS-190 latex surfaces is shown. The switch to either of the new polyelectrolytes is

Table 3 Particle diameters, ζ-potentials, and functional groups of the colloids

Particle	Diameter (nm)	ζ-Potential (mV) in 10^{-3} M NaCl	Functional group
NaSS-190 latex	190	− 50 (pH 4)	SO_3^-
DEAM-250 latex	252	+ 60 (pH 4)	$\rangle NH^+$
PS-740 latex	740	− 30 (pH 4)	OSO_3^-
Silica-500	500	− 30 (pH 6)	SiO_2^-
Silica-300	300	− 30 (pH 6)	SiO_2^-
Silica-20	20	− 30 (pH 6)	SiO_2^-

MARCEL DEKKER, INC.
270 Madison Avenue, New York, New York 10016

indicated by the arrows. In the figure, the abscissa axis indicates the total number of repeating units of both polyelectrolyte molecules. The change of the ζ-potential is substantial (i.e., the ζ-potential is highly positive after the addition of PLL-19 and highly negative after the addition of PSSNa-50). This result indicates clearly that, on the adsorption of polyelectrolyte, the oppositely charged surface is not just compensated but strongly overcompensated. An overcompensation of polyelectrolyte adsorption is the main reason for progressing the multilayer formation. The buildup process was also confirmed from the stepwise increase of the layer thickness of the core latex particles. The stepwise increase of the layer thickness, especially after the adsorption of PSSNa-50 molecules on the core particle surfaces, is also shown in Fig. 17.

In the next stage, we tried to produce polyelectrolyte multilayers under different medium compositions. In Fig. 18, the results of multilayer formations of PSSNa-50 and PLL-19 in pure water at pH 4, 10^{-2} M NaCl solution, and 10^{-2} M $BaCl_2$ solution are indicated. In these experiments, the positively charged DEAM-250 lattices were used as the core particles. In this figure, the

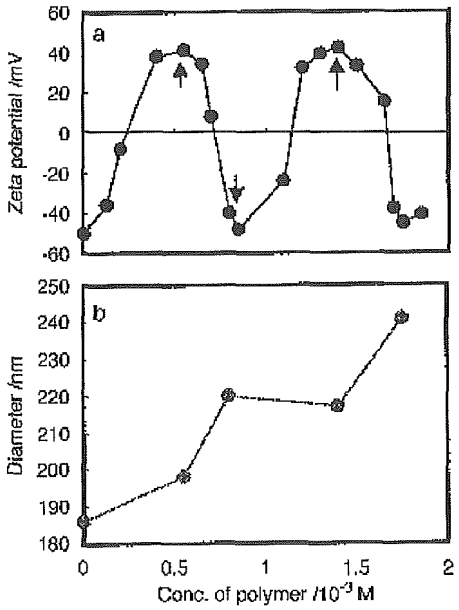

Fig. 17 ζ-Potential (a) and total particle size (b) of the composite system by multilayer deposition of PLL-19 and PSSNa-50 on NaSS-10 lattices against the concentrations of each polyelectrolyte solution (ϕ = 7.5 × 10^{-3} wt.%, pH 4, [NaCl] = 1 × 10^{-3} M). The switch to a new polymer solution is indicated by the arrows.

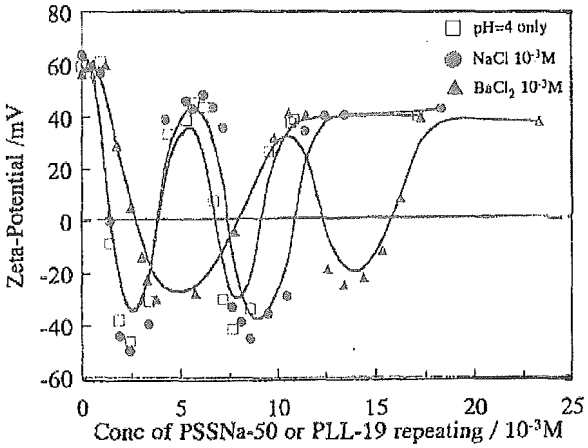

Fig. 18 ζ-Potential of multilayers of PSSNa-50 and PLL-19 on DEAM-250 lattices against the concentrations of each polyelectrolyte solution under different salt conditions (ϕ = 7.5 × 10^{-3} wt.%, pH 4).

locus of ζ-potentials obtained under different salt conditions is plotted for the total amounts of repeating units of PLL-19 and PSSNa-50 molecules. As can be seen, the step in the ζ-potential obtained in the $BaCl_2$ solution is delayed, indicating that the electrostatic attraction between PSSNa-50 and the charged surface of DEAM-250 lattices is weakened. This is caused by the strong affinity of Ba^{2+} to SO_3^- in PSSNa-50 molecules. The existence of such a specific effect has been reported in the literature.[37,38]

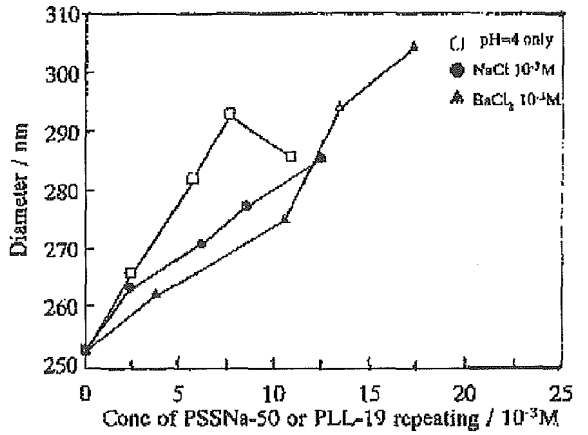

Fig. 19 The total particle sizes in each step to stable multilayers of PSSNa-50 and PLL-19 on DEAM-250 lattices under different salt conditions (ϕ = 7.5 × 10^{-3} wt.%, pH 4).

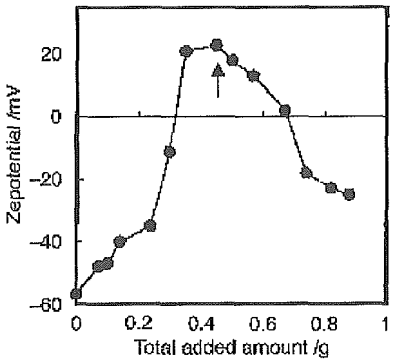

Fig. 20 ζ-Potential of composite particles by multilayer deposition of PLL-19 (concentration, 2×10^{-4} wt.%) and Silica-300 (concentration, 1.0×10^{-3} wt.%) on PS-740 lattices ($=7.5 \times 10^{-4}$ wt.%, pH 6, [NaCl]$=1 \times 10^{-3}$ M). The switch to Silica-300 from PLL-19 is indicated by the arrow.

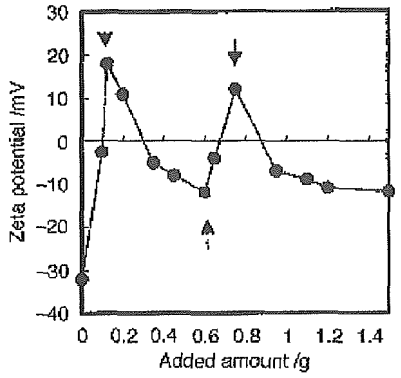

Fig. 22 ζ-Potential of composite particles by multilayer deposition of pair (PLL-19 + Silica-20) layers. The switch is indicated by the arrow.

Fig. 19 indicates the stepwise increase of layer thickness on DEAM-250 latex particles under different salt conditions. Surprisingly, in the 10^{-2} M $BaCl_2$ solutions, the layer thickness of adsorbed polyelectrolytes increased steadily and the weak attraction effect coming from Ba^{2+} was not observed on the layer-by-layer formation. However, in distilled water, the layer thickness increased quickly at an early stage of deposition. However, in the final stage, the layer shrunk. The reason for this phenomenon cannot be explained, but this result indicates surely that strong electrostatic attraction is not always the sole factor necessary to form a stable multilayer.

Multilayer formation of colloid particles with polyelectrolytes

The layer-by-layer deposition technique of polyelectrolytes can be applied to the formation of composite particles comprising organic and inorganic colloid particles.

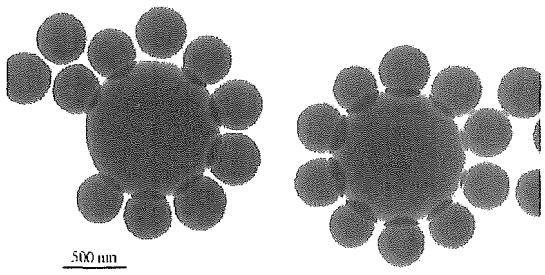

Fig. 21 Electron micrograph showing hybrid particles of outer Silica-300 particles on core PS-740 lattices.

Fig. 20 shows the buildup processes of colloid particles using PS-740 latex sample as the core. Here, PLL-19 was used as a binder polyelectrolyte. The abscissa axis in this figures indicates the total amounts of the binder polyelectrolyte + adhering particles. As can be seen from the figure, the ζ-potential of the core particle has changed from a negative value to a positive value by adsorption of PLL-19 molecules, and changed again to negative values with an increasing number of adhering silica particles (Silica-300). These results suggest that the composite formation of colloid particles has progressed reasonably by the binder layer of PLL-19 molecules. Fig. 21 is a photograph showing a typical example of hybrid particles consisting of outer Silica-300 particles on core PS-740 latex as prepared in this experiment. It is known that the composite consists of regular hybrid particles comprising organic and inorganic particles. However, the structure form is not so stable and sometimes the system includes free silica particles.

In the next stage, the synthetic process of hybrid particles with multilayers of silica particles on PS-740 was examined. As the binder polyelectrolyte, the PLL-19 molecule was also used under the same medium conditions. Fig. 22 shows the cyclical behavior of the ζ-potential in the formation process of multilayers of Silica-20 and PLL-19 layers. As can be seen, the cycle of ζ-potential after adhesion is systematical, indicating that the deposition of PLL and Silica-20 has progressed regularly. Fig. 23 is a photograph of an original PS-740 latex and two kinds of composite particles covered with a single silica + polymer layer and two silica + polymer layers. Two kinds of composite particles can be distinguished based on the thickness of the adhering silica particle layer.